World Conference on Social Sciences, Law and Public Policy
Hosted Online from Toronto, Canada
Date: 26th June 2026
Website: https://econferencia.com

INVESTIGATION OF THE MAGNETIC CIRCUITS OF A NEW TRANSFORMER-BASED RESONANT SENSOR FOR MOTION PARAMETER MEASUREMENT

Mukhtorov U. B.
Tashkent State Transport University,
1 Temiryulchilar Street, Tashkent 100167, Uzbekistan

Abstract

This paper investigates the linear and nonlinear distributed-parameter circuits of a new resonant transformer sensor intended for converting motion parameters (displacement and velocity) into electrical signals. It is shown that in the linear distributed-parameter circuit of the sensor, the magnetic flux and magnetic field intensity vary along the length of the circuit according to a nonlinear law; moreover, the degree of this nonlinearity increases with an increase in the attenuation coefficient of the magnetic field along the magnetic circuit. When the distributed-parameter magnetic circuit of the sensor operates in the nonlinear regime, achieving a linear distribution of the working magnetic flux along the circuit length requires that the working air gap between adjacent long ferromagnetic rods vary along the length of the circuit according to a prescribed law. In this case, the magnitude of the variation of the working magnetic flux along the circuit length does not depend on the value of the approximation coefficient characterizing the nonlinearity of the circuit. The magnetic field intensity between adjacent long ferromagnetic rods of a nonlinear distributed-parameter magnetic circuit decreases according to a nonlinear law from the region where the magnetomotive force source is located toward the end of the circuit, and the rate of this decrease increases with an increase in the value of the approximation coefficient characterizing the circuit nonlinearity.

Keywords: transformer sensor, resonance, linear magnetic circuit, nonlinear magnetic circuit, distributed parameters, magnetic flux, magnetic field intensity, magnetic reluctance, magnetic capacitance, main magnetization curve, analytical method, differential equations, long ferromagnetic rods, approximation, working air gap.

Introduction

Transformer sensors designed for measuring electrical and non-electrical quantities constitute one of the fundamental functional elements of modern monitoring and control systems [1,2]. These sensors are extensively employed in electrical engineering, power engineering, and industrial automation, where they convert physical quantities into electrical signals. Among various types of transformer sensors, resonant transformer sensors intended for motion parameter measurements are distinguished by their high sensitivity and measurement accuracy [3,4].

An additional advantage of resonant transformer sensors is their relatively high output power and strong immunity to external disturbances. These characteristics ensure reliable operation even under harsh environmental and operating conditions. Furthermore, their principal metrological characteristics remain stable over extended periods of service, allowing compliance with established technical standards and regulatory requirements. Consequently, resonant transformer sensors are widely utilized in automated monitoring and control systems requiring high accuracy, long-term stability, and operational reliability [5–7].

At Tashkent State Transport University, two novel designs of resonant transformer sensors capable of simultaneously converting motion parameters (linear displacement and velocity) into electrical signals have recently been developed [8,9]. The present study focuses on the investigation of the magnetic circuit of one of these sensors (Fig. 1). A detailed description of the sensor structure, operating principle, and its advantages over the prototype has been presented in [9]. Therefore, these aspects are not discussed further in this paper.

The proposed sensor incorporates a distributed-parameter magnetic circuit (DPMC), in which the magnetic reluctances of elongated ferromagnetic rods and the magnetic permeances of the working air gaps between adjacent rods are continuously distributed along the magnetic circuit length according to the classical analogy between electrical and magnetic circuits. The distribution of the working magnetic flux along the ferromagnetic rods significantly affects the resonance conditions of the electrical circuit and determines the shape of the static transfer characteristic. Therefore, determining the magnetic flux distribution within the distributed magnetic circuit is an essential stage in the design and optimization of the proposed resonant transformer sensor.

Since the investigated magnetic circuit belongs to the class of distributed-parameter magnetic circuits, the following assumptions are adopted to simplify the analysis: 1. The ferromagnetic core operates within the linear region of the primary magnetization curve; this assumption is valid for the initial stage of the analysis. 2. Magnetic leakage fluxes through the lateral surfaces, ends, and edges of the magnetic core are neglected. 3. The axial dimensions of the excitation and measuring windings are assumed to be negligible compared with the length of the magnetic circuit. 4. The distributed magnetic parameters are assumed to be uniformly distributed along the magnetic circuit.

As reported in [10,11], these assumptions have only a minor influence on the calculation accuracy while substantially simplifying the mathematical analysis of the distributed-parameter magnetic circuit.

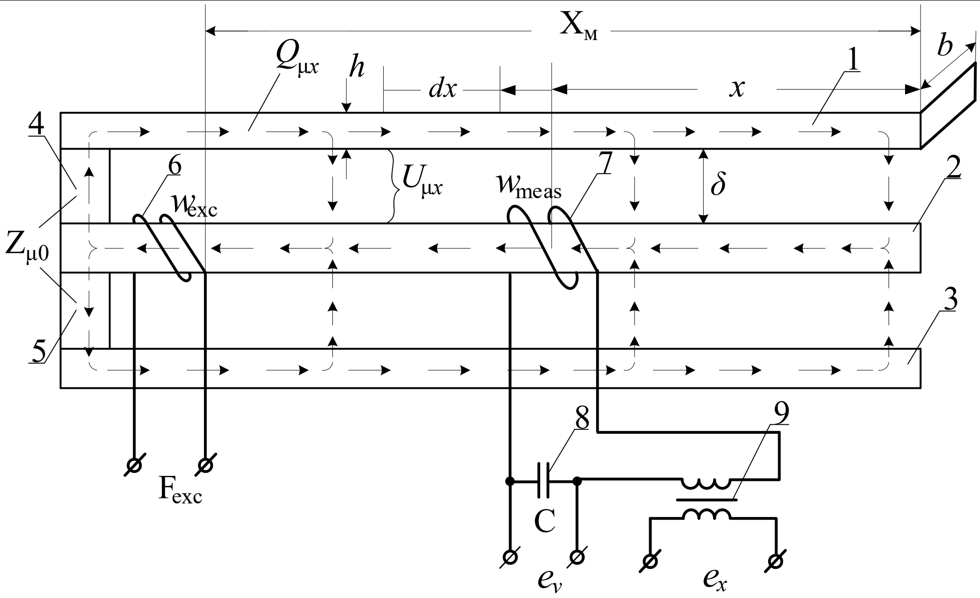

Fig. 1. Schematic diagram of the proposed resonant transformer sensor for motion parameter measurement: (1–3) elongated ferromagnetic rods; (4, 5) ferromagnetic yokes; (6) excitation winding; (7) measuring winding; (8) capacitor; (9) transformer.

A comparative analysis of the existing methods for calculating linear distributed-parameter magnetic circuits (DPMCs) indicates that the most suitable approach for analyzing the magnetic circuit of the proposed transformer sensor is the classical method based on the formulation and solution of differential equations describing the transformer processes in the distributed-parameter magnetic circuit [12,13].

For the analysis of the investigated DPMC, it is convenient to define the origin of the coordinate x at the open end of the elongated ferromagnetic rods, where the concentrated movable winding is located. Since the DPMC is symmetric with respect to the axis of the central ferromagnetic rod, it is sufficient to analyze only one half of the magnetic circuit. Therefore, in this study, the upper half of the magnetic circuit is considered, and the working magnetic flux as well as the magnetic potential difference between elongated ferromagnetic rods 1 and 2 are determined.

Based on Kirchhoff's laws, the following differential equations describing the magnetic flux ($\mathrm{Q_{\mu x}}$) in the parallel ferromagnetic rods and the magnetic potential difference ($\mathrm{U_{\mu x}}$) between them are formulated for an infinitesimal element dx of the magnetic circuit [10,11] (Fig. 2):

$$\dot{\mathrm{Q}}_{\mu x} + \mathrm{d}\dot{\mathrm{Q}}_{\mu x} - \dot{\mathrm{U}}_{\mu x}\mathrm{C}_{\mu p}\mathrm{dx} - \dot{\mathrm{Q}}_{\mu x} = 0 \quad \text{or} \quad \frac{\mathrm{d}\dot{\mathrm{Q}}_{\mu x}}{\mathrm{dx}} = \dot{\mathrm{U}}_{\mu x}\mathrm{C}_{\mu p}, \qquad (1)$$

$$-\dot{\mathrm{U}}_{\mu x} - \mathrm{d}\dot{\mathrm{U}}_{\mu x} + \underline{\mathrm{Z}}_{\mu p}\dot{\mathrm{Q}}_{\mu x}\mathrm{dx} + \dot{\mathrm{U}}_{\mu x} + \underline{\mathrm{Z}}_{\mu p}\dot{\mathrm{Q}}_{\mu x}\mathrm{dx} = 0 \quad \text{or} \quad \frac{\mathrm{d}\dot{\mathrm{U}}_{\mu x}}{\mathrm{dx}} = 2\underline{\mathrm{Z}}_{\mu p}\dot{\mathrm{Q}}_{\mu x}, \qquad (2)$$

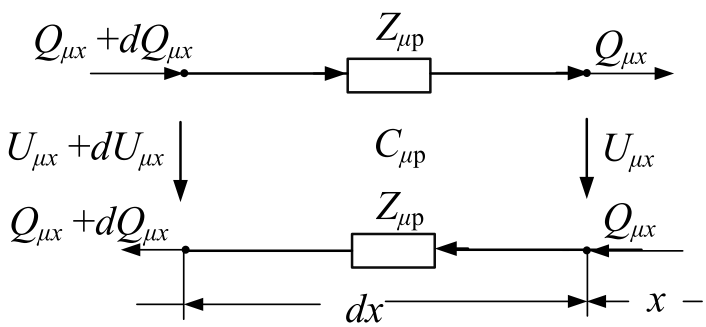

Fig. 2. Equivalent circuit of an elementary section of the distributed-parameter magnetic circuit (DPMC) with a length of dx

here, $\underline{\mathrm{Z}}_{\mu p} = \frac{1}{\mu\mu_0 \mathrm{bh}}, [\mathrm{H^{-1} \cdot m^{-1}}]$; $\mathrm{C}_{\mu p} = \mu_0 \frac{\mathrm{b}}{\delta}, [\mathrm{H \cdot m^{-1}}]$, where $\underline{\mathrm{Z}}_{\mu p}$ and $\mathrm{C}_{\mu p}$ are the per-unit-length values of the complex magnetic reluctance of the elongated ferromagnetic rods and the magnetic permeance of the air gap between two adjacent rods, respectively. The geometric dimensions of the distributed-parameter magnetic circuit are shown in Fig. 1.

Differentiating Eq. (2) with respect to x and substituting the result into Eq. (1) yields the following second-order linear differential equation:

$$\frac{d^2\dot{U}_{\mu x}}{dx^2} = 2\underline{Z}_{\mu p}C_{\mu p}\dot{U}_{\mu x}. \tag{3}$$

The general solution of the differential equation (3) can be expressed in the following form [14]:

$$\dot{U}_{\mu x} = \underline{A}_1 e^{\underline{\gamma} x} + \underline{A}_2 e^{-\underline{\gamma} x}, \tag{4}$$

here $\underline{\gamma} = \sqrt{2\underline{Z}_{\mu p}C_{\mu p}}$, $[m^{-1}]$ - magnetic field propagation coefficient along the magnetic circuit; $\underline{A}_1, \underline{A}_2$ - integration constants, [A].

Differentiating Eq. (4) with respect to (x) and substituting the resulting expression into Eq. (2), the following expression for the magnetic flux $\dot{Q}_{\mu x}$ is obtained:

$$\dot{Q}_{\mu x} = \frac{\underline{\gamma}}{2\underline{Z}_{\mu p}}\underline{A}_1 e^{\underline{\gamma} x} - \frac{\underline{\gamma}}{2\underline{Z}_{\mu p}}\underline{A}_2 e^{-\underline{\gamma} x}. \tag{5}$$

The integration constants $\underline{A}_1, \underline{A}_2$ are determined by applying the following boundary conditions corresponding to the investigated distributed-parameter magnetic circuit:

$$\dot{Q}_{\mu x=0} = 0; \ \dot{U}_{\mu x = X_M} = \dot{F}_{exc} - \underline{Z}_{\mu 0}\dot{Q}_{\mu x = X_M}, \tag{6}$$

here $\dot{F}_{exc}$- complex value of the magnetomotive force (MMF) of the excitation winding, [A]; $\underline{Z}_{\mu 0}$ – magnetic reluctance of the ferromagnetic yoke $[H^{-1}]$; X_M - maximum value of the coordinate x.

Substituting the values of the magnetic flux and the magnetic potential difference at the cross-sections corresponding to the boundary conditions into Eq. (6) yields the following system of algebraic equations with respect to the unknown integration constants $\underline{A}_1$, $\underline{A}_2$

$$\begin{cases} \dfrac{\underline{\gamma}}{2\underline{Z}_{\mu p}}\underline{A}_1 - \dfrac{\underline{\gamma}}{2\underline{Z}_{\mu p}}\underline{A}_2 = 0, \\ \left(1 + \dfrac{\underline{\gamma}\underline{Z}_{\mu 0}}{2\underline{Z}_{\mu p}}\right) e^{\underline{\gamma} X_M}\underline{A}_1 + \left(1 - \dfrac{\underline{\gamma}\underline{Z}_{\mu 0}}{2\underline{Z}_{\mu p}}\right) e^{-\underline{\gamma} X_M}\underline{A}_2 = 0. \end{cases} \tag{7}$$

Solving the system of equations (7) yields the following expressions for the integration constants appearing in Eqs. (4) and (5):

$$\underline{A}_1 = \frac{\dot{F}_{exc}\underline{Z}_{\mu p}}{2\underline{Z}_{\mu p}\mathrm{ch}\left(\underline{\gamma}X_{\text{м}}\right) + \underline{\gamma}\underline{Z}_{\mu 0}\mathrm{sh}\left(\underline{\gamma}X_{\text{м}}\right)}, \tag{8}$$

$$\underline{A}_2 = \frac{\dot{F}_{exc}\underline{Z}_{\mu p}}{2\underline{Z}_{\mu p}\mathrm{ch}\left(\underline{\gamma}X_{\text{м}}\right) + \underline{\gamma}\underline{Z}_{\mu 0}\mathrm{sh}\left(\underline{\gamma}X_{\text{м}}\right)}, \tag{9}$$

here $\underline{\Delta}= 2\underline{Z}_{\mu p}\mathrm{ch}\left(\underline{\gamma}X_{\text{м}}\right) + \underline{\gamma}\underline{Z}_{\mu 0}\mathrm{sh}\left(\underline{\gamma}X_{\text{м}}\right)$, $[\mathrm{H}^{-1}\cdot \mathrm{m}^{-1}]$.

Taking Eqs. (8) and (9) into account, the magnetic flux in the elongated ferromagnetic rod 1 and the magnetic potential difference between the adjacent rods at the cross-section with coordinate x are determined as follows:

$$\dot{U}_{\mu x} = \frac{2\dot{F}_{exc}\underline{Z}_{\mu p}\mathrm{ch}\left(\underline{\gamma}x\right)}{\underline{\Delta}}, \tag{10}$$

$$\dot{Q}_{\mu x} = \frac{\underline{\gamma}\dot{F}_{exc}\mathrm{sh}\left(\underline{\gamma}x\right)}{\underline{\Delta}}. \tag{11}$$

For convenience of analysis, Eqs. (10) and (11) are expressed in normalized form using per-unit values, and their corresponding distributions are presented in Fig. 3.

$$U^*_{\mu x^*} = \frac{U_{\mu x^*}}{U_{\mu(x^*=1)}} = \frac{\mathrm{ch}\left(\underline{\beta}x^*\right)}{\mathrm{ch}(\underline{\beta})} \tag{12}$$

$$Q^*_{\mu x^*} = \frac{Q_{\mu x^*}}{Q_{\mu(x^*=1)}} = \frac{\mathrm{sh}(\underline{\beta}x^*)}{\mathrm{sh}(\underline{\beta})} \tag{13}$$

here $\underline{\beta} = \underline{\gamma}X_{\text{м}}$, $[-]$ - attenuation coefficient of the magnetic field along the distributed-parameter magnetic circuit (DPMC); $x^* = x/X_{\text{м}}$ $[-]$.

Analysis of Eqs. (10) and (11), together with the corresponding plots obtained for different values of β, indicates that the magnetic flux and the magnetic potential difference in the investigated linear distributed-parameter magnetic circuit are distributed nonlinearly along the length of the magnetic circuit. Furthermore, the degree of this nonlinearity increases with an increase in the magnetic field attenuation coefficient β.

It should be noted that the magnetic induction in the elongated ferromagnetic rods of the investigated distributed-parameter magnetic circuit reaches its maximum value in the region adjacent to the magnetomotive force (MMF) source and gradually decreases toward the open ends of the rods. Therefore, an analysis of the actual magnetic field distribution reveals that the magnetic induction in the elongated ferromagnetic rods varies over a wide range, $B_{max} \leq B \leq B_{min} \approx 0$

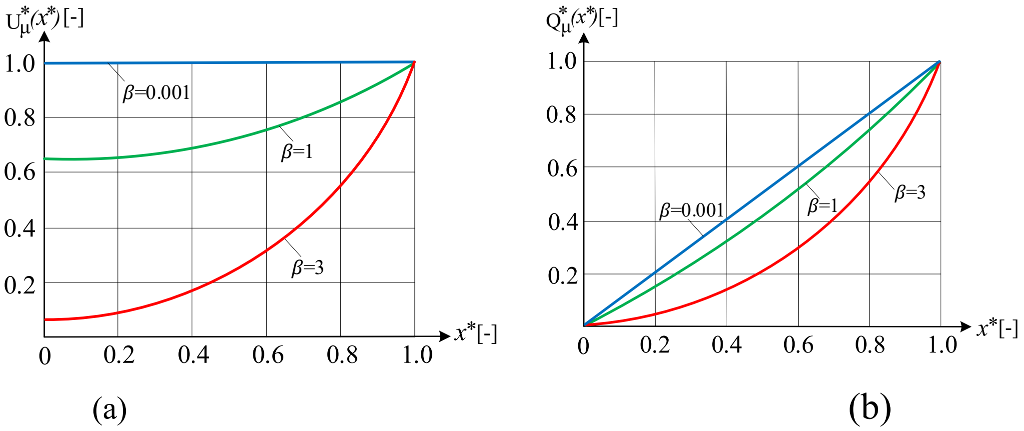

Fig. 3. Distributions of the normalized functions $Q^*_{\mu x^*} = f(x^*)$ (a) and $U^*_{\mu x^*} = f(x^*)$ (b) for different values of the magnetic field attenuation coefficient β.

Considering that the maximum magnetic induction in transformer sensors is typically within the range of $1{,}2 \leq B_{max} \leq 1{,}6\,T$ [10,11], modeling the investigated distributed-parameter magnetic circuit as a linear system may result in significant errors of approximately (40%-70%). Therefore, under such conditions, it is appropriate to account for the nonlinear magnetization characteristic of the ferromagnetic material in the magnetic core when analyzing the distributed-parameter magnetic circuit.

A comparative analysis of the existing methods for investigating nonlinear distributed-parameter magnetic circuits (DPMCs) shows that the differential equations describing such circuits are generally solved using numerical, i.e., approximate, methods [13]. Consequently, the accuracy of the obtained results is inevitably reduced.

Therefore, in the present study, the nonlinear distributed-parameter magnetic circuit is analyzed using an analytical method that enables an exact solution of the nonlinear differential equations describing the transformer processes in the circuit [15]. Another important advantage of this method is that, in addition to providing an exact analytical solution, it makes it possible to determine the variation law of a geometric parameter or the per-unit number of turns of a distributed excitation winding along the magnetic circuit, thereby ensuring a linear distribution of the working magnetic flux, which is required for most transformer sensors.

It is well known [16,17] that the investigation of nonlinear distributed-parameter magnetic circuits requires an analytical approximation of the magnetization characteristic of the ferromagnetic material. In transformer sensors, the magnetic cores are generally manufactured from magnetically soft electrical steels whose hysteresis loop area is sufficiently small to be neglected [18]. Therefore, for engineering calculations, it is sufficient to approximate only the primary magnetization curve.

Studies devoted to the approximation of the primary magnetization curve and the evaluation of the effectiveness of various approximation functions for nonlinear distributed-parameter magnetic circuits have shown that the incomplete polynomial $H = pB + qB^3$ provides the most suitable approximation for the above analytical method while ensuring sufficient accuracy for engineering applications [19].

According to the analytical method proposed in [15], the system of nonlinear differential equations is supplemented by the condition that the second derivative of the magnetic flux with respect to the magnetic circuit length is equal to zero. Simultaneously, one of the distributed parameters characterizing the magnetic circuit, such as the air-gap length between adjacent ferromagnetic rods, the rod thickness, the rod width, or the number of turns per unit length of the distributed excitation winding, is assumed to be a function of the coordinate along the magnetic circuit. These assumptions considerably simplify the original system of equations and make it possible to obtain exact analytical expressions describing the distribution of the magnetic flux and magnetic potential difference along the magnetic circuit.

In the present study, the nonlinear distributed-parameter magnetic circuit is analyzed using the above analytical method by assuming that the working air-gap length between adjacent elongated ferromagnetic rods is a function of the coordinate x, i.e. $\delta_x = f(x)$

The differential equations describing the distributions of the magnetic flux and the magnetic potential difference along the magnetic circuit for an infinitesimal element dx of the investigated nonlinear distributed-parameter magnetic circuit can therefore be written in the following form:

$$\dot{Q}'_{\mu x} = \dot{U}_{\mu x} C_{\mu p x} = \dot{U}_{\mu x}\mu_0 \frac{b}{\delta_x} = k_1 \, \dot{U}_{\mu x}/\delta_x, \qquad (14)$$

$$\dot{U}'_{\mu x} = 2\underline{Z}_{\mu p}\,(\dot{Q}_{\mu x})\dot{Q}_{\mu x} = 2\rho_{\mu}(\dot{Q}_{\mu x})\frac{\dot{Q}_{\mu x}}{bh} =$$

$$= 2\left(p + q\frac{\dot{Q}^2_{\mu x}}{b^2h^2}\right)\frac{\dot{Q}_{\mu x}}{bh} = k_2\dot{Q}_{\mu x} + k_3\dot{Q}^3_{\mu x}, \qquad (15)$$

here $\rho_\mu(\dot{Q}_{\mu x}) = p + q\frac{\dot{Q}^2_{\mu x}}{b^2h^2}, [H^{-1}\cdot m]$ – specific magnetic reluctance of the magnetic core material [15]; p, q – approximation coefficients; $k_1 = \mu_0 b, [H]$; $k_2 = 2p/bh, [H^{-1}\cdot m^{-1}]$; $k_3 = 2q/(b^3h^3), [H^{-1}\cdot T^{-2}\cdot m^{-5}]$;

For the investigated nonlinear distributed-parameter magnetic circuit, the following boundary conditions are applied, assuming that the magnetic reluctance at the end where the excitation winding is located is $\underline{Z}_{\mu 0}$, while the magnetic reluctance at the open end of the circuit is infinitely large, i.e., $\underline{Z}_{\mu in} = \infty$. The origin of the coordinate x is taken at the open end of the magnetic circuit:

$$\dot{Q}_{\mu x=0} = 0;\ \delta_{x=0} = \delta_0;\ \dot{U}_{\mu x=X_М} = \dot{F}_{exc} - \underline{Z}_{\mu 0}(\dot{Q}_{\mu x})\cdot \dot{Q}_{\mu x=X_М}, \tag{16}$$

here $\underline{Z}_{\mu 0}(\dot{Q}_{\mu x}) = \frac{p}{bh} + q\frac{\dot{Q}^2_{\mu x=X_М}}{b^3h^3}, [H^{-1}]$.

Anecessary and sufficient condition for achieving a linear distribution of the magnetic flux along the distributed-parameter magnetic circuit is that its second derivative with respect to the coordinate x be equal to zero, i.e.[Konyukhov, p. 20]:

$$\dot{Q}''_{\mu x} = 0. \tag{17}$$

Integrating the differential equation (17) twice yields the following expression:

$$\dot{Q}_{\mu x} = \underline{A}_1 x + \underline{A}_2. \tag{18}$$

If the initial condition given by Eq. (16) is taken into account, then $\underline{A}_2 = 0$, and Eq. (18) can be rewritten in the following form:

$$\dot{Q}_{\mu x} = \underline{A}_1 x. \tag{19}$$

It follows from Eq. (19) that $\dot{Q}'_{\mu x} = \underline{A}_1 = const$, (20)

Determining $\dot{U}_{\mu x}$ from Eq. (14), substituting Eq. (20) into the resulting expression, and differentiating it with respect to **x** yields the following two equations:

$$\dot{U}_{\mu x} = \left(\underline{A}_1/k_1\right)\delta_x, \quad (21) \qquad \dot{U}'_{\mu x} = \left(\underline{A}_1/k_1\right)\delta'_x. \quad (22)$$

Equating the right-hand side of the equation obtained by substituting Eq. (19) into Eq. (15) with the right-hand side of Eq. (22), the derivative δ'_x is obtained as follows:

$$\delta'_x = k_1\left(k_2 x + k_3 \underline{A}_1^2 x^3\right). \qquad (23)$$

Integrating the differential equation (23) yields the following general solution for δ_x:

$$\delta_x = \frac{k_1 k_2}{2} x^2 + \frac{k_1 k_3}{4} \underline{A}_1^2 x^4 + \underline{A}_3. \qquad (24)$$

Substituting the second boundary condition given in Eq. (16) into Eq. (24) yields the integration constant $\underline{A}_3 = \delta_0$. Substituting this result back into Eq. (24) gives the following expression:

$$\delta_x = \delta_0 + \frac{k_1 k_2}{2} x^2 + \frac{k_1 k_3}{4} \underline{A}_1^2 x^4. \qquad (25)$$

Substituting Eq. (25) into Eq. (21) yields the following expression:

$$\dot{U}_{\mu x} = \frac{\underline{A}_1}{k_1}\left(\delta_0 + \frac{k_1 k_2}{2} x^2 + \frac{k_1 k_3}{4} \underline{A}_1^2 x^4\right). \qquad (26)$$

Substituting the third boundary condition given in Eq. (16) into Eq. (26) yields the following third-order algebraic equation with respect to $\underline{A}_1$:

$$\left(\frac{k_3 X_{\text{М}}^4}{4} + k_5 X_{\text{М}}^3\right)\underline{A}_1^3 + \left(\frac{\delta_0}{k_1} + \frac{k_2 X_{\text{М}}^2}{2} + k_4 X_{\text{М}}\right)\underline{A}_1 - \dot{F}_{exc} = 0, \qquad (27)$$

here $k_4 = p$; $k_5 = q/(b^2 h^2), [H^{-1} \cdot T^{-2} \cdot m^{-3}]$.

Equation (27) can be solved using existing analytical techniques, such as Cardano's method [14]. The analysis shows that, for the parameter values of the investigated nonlinear distributed-parameter magnetic circuit, the discriminant of Eq. (27) is positive. Consequently, the equation has the following unique real solution:

$$\underline{A}_1 = \sqrt[3]{\frac{\dot{F}_{exc}}{2a} + \sqrt{\left(\frac{\dot{F}_{exc}}{2a}\right)^2 + \left(\frac{d}{3a}\right)^3}} + \sqrt[3]{\frac{\dot{F}_{exc}}{2a} - \sqrt{\left(\frac{\dot{F}_{exc}}{2a}\right)^2 + \left(\frac{d}{3a}\right)^3}}, \quad (28)$$

here $a = \frac{k_3 X_{\text{M}}^4}{4} + k_5 X_{\text{M}}^3$, $d = \frac{\delta_0}{k_1} + \frac{k_2 X_{\text{M}}^2}{2} + k_4 X_{\text{M}}$.

For convenience of analysis, Eqs. (19) and (26) are expressed in normalized (per-unit) form as follows, and their corresponding distributions are presented in Fig. 4.

$$U_{\mu x^*}^* = \frac{U_{\mu x^*}}{U_{\mu(x^*=1)}} = \frac{\delta_0 + \frac{k_1 k_2 X_{\text{M}}^2}{2}(x^*)^2 + \frac{k_1 k_3 X_{\text{M}}^4}{4}\underline{A}_1^2 (x^*)^4}{\delta_0 + \frac{k_1 k_2 X_{\text{M}}^2}{2} + \frac{k_1 k_3 X_{\text{M}}^4}{4}\underline{A}_1^2}, \quad (29)$$

$$Q_{\mu x^*}^* = \frac{Q_{\mu x^*}}{Q_{\mu(x^*=1)}} = x^*. \quad (30)$$

Analysis of Eqs. (19) and (25), derived for the nonlinear distributed-parameter magnetic circuit of the proposed transformer sensor, together with the plots of the normalized function $Q_{\mu x^*}^* = f(x^*)$ constructed from Eq. (19) for different values of the approximation coefficient, shows that a linear distribution of the working magnetic flux along the magnetic circuit can be achieved only if the working air gap between the adjacent elongated ferromagnetic rods varies along the circuit according to Eq. (25). Furthermore, the distribution of the working magnetic flux along the magnetic circuit is independent of the value of the approximation coefficient q, which characterizes the nonlinearity of the magnetic circuit.

An analysis of Eq. (26) and the corresponding plots of the normalized function $U_{\mu x^*}^* = f(x^*)$ obtained for different values of the approximation coefficient shows that the magnetic potential difference between the adjacent elongated ferromagnetic rods decreases nonlinearly from the section containing the magnetomotive force (MMF) source toward the open end of the magnetic circuit. Moreover, the degree of this nonlinearity increases with increasing values of the approximation coefficient q, which characterizes the nonlinear properties of the magnetic circuit.

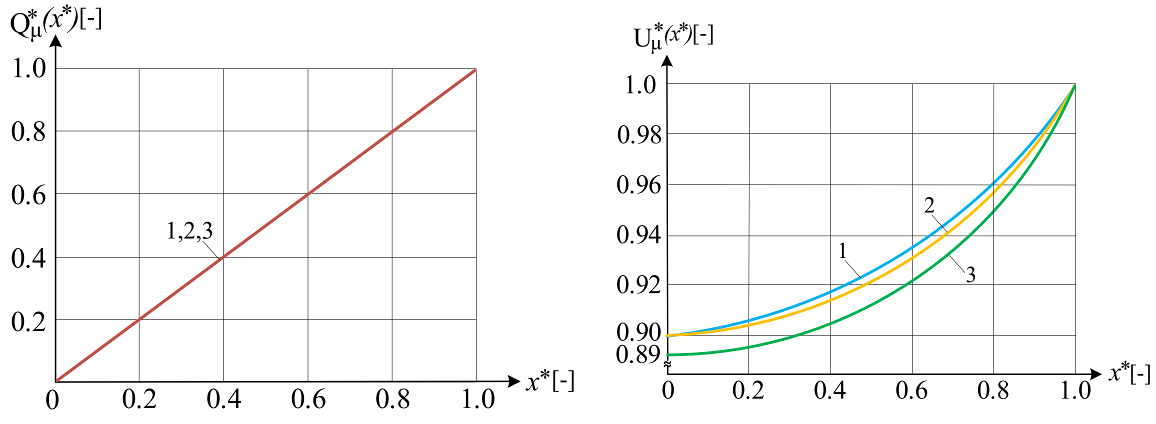

(a)

(b)

Fig. 4. Plots of the normalized functions $Q^*_{\mu x^*} = f(x^*)$ (a) and $U^*_{\mu x^*} = f(x^*)$ (b) for different values of the approximation coefficients (p) and (q). $1 - p = 800, q = 500\ (0.4 \le B \le 0.6\ T); 2 - \ p = 700, q = 1200\ (0.4 \le B \le 0.8\ T); 3 - \ p = 600, q = 2500\ (0.4 \le B \le 1.0\ T)$.

The above analysis demonstrates that when the primary magnetization curve (PMC) of the magnetic core material in the nonlinear distributed-parameter magnetic circuit is approximated by the incomplete polynomial $H = pB + qB^3$ the resulting nonlinear differential equation of the distributed-parameter magnetic circuit admits an exact analytical solution when solved using the analytical method proposed in [15].

Next, we investigate the applicability of the same analytical method [15] when the primary magnetization curve is approximated by the hyperbolic sine and tangent functions, which are widely used in magnetic circuit analysis: $H = \alpha sh(\beta B)$ and ($H = \alpha tg(\beta B)$)

When the primary magnetization curve is approximated by the hyperbolic sine function, $H = \alpha sh(\beta B)$, Eq. (14) remains unchanged, whereas Eq. (15) takes the following form:

$$\dot{U}'_{\mu x} = 2\underline{Z}_{\mu p}\left(\dot{Q}_{\mu x}\right)\dot{Q}_{\mu x} = 2\rho_{\mu}\left(\dot{Q}_{\mu x}\right)\frac{\dot{Q}_{\mu x}}{bh} = \alpha_1 sh\left(\beta_1 \dot{Q}_{\mu x}\right), \tag{31}$$

here $k_1 = \mu_0 b, [H]$; $\alpha_1 = 2\alpha$, $\beta_1 = \frac{\beta}{bh}$;. $l_{\mu 0} = \delta_{x=X_{\text{M}}}$.

Assuming that $\delta_x = f(x)$, and solving Eqs. (14), (16), and (31) simultaneously with the condition $\dot{Q}''_{\mu x} = 0$, the following solutions are obtained:

$$\dot{Q}_{\mu x} = \underline{A}_1 x, \tag{32}$$

$$\delta_x = \delta_0 + \frac{k_1}{\underline{A}_1^2}\cdot\frac{\alpha_1}{\beta_1}\left[ch\left(\beta_1 \underline{A}_1 x\right) - 1\right], \tag{33}$$

$$\dot{U}_{\mu x} = \frac{\underline{A}_1}{k_1}\left(\delta_0 + \frac{k_1}{\underline{A}_1^2}\cdot\frac{\alpha_1}{\beta_1}\left[ch\left(\beta_1 \underline{A}_1 x\right) - 1\right]\right). \tag{34}$$

Substituting the third boundary condition given in Eq. (16) into Eq. (33) yields the following third-order algebraic equation with respect to $\underline{A}_1$:

$$\frac{\underline{A}_1}{k_1}\delta_0 + \frac{\alpha_1}{\underline{A}_1\beta_1}\left[ch\left(\beta_1 \underline{A}_1 X_{\text{M}}\right) - 1\right] + \alpha l_{\mu 0} sh\left(\beta_1 \underline{A}_1 X_{\text{M}}\right) - \dot{F}_{exc} = 0 \tag{35}$$

Equation (35) is a transcendental equation, which has no closed-form analytical solution. Therefore, the unknown parameter $\underline{A}_1$ must be determined using numerical methods, and the resulting solution is approximate.

Similarly, when the primary magnetization curve is approximated by the tangent function, $H = \alpha tg(\beta B)$, Eq. (14) remains unchanged, whereas Eq. (15) can be written in the following form:

$$\dot{U}'_{\mu x} = 2\underline{Z}_{\mu p}(\dot{Q}_{\mu x})\dot{Q}_{\mu x} = 2\rho_{\mu}(\dot{Q}_{\mu x})\frac{\dot{Q}_{\mu x}}{bh} = \alpha_1 tg(\beta_1 \dot{Q}_{\mu x}). \quad (36)$$

Assuming that $\delta_x = f(x)$, and solving Eqs. (14), (16), and (36) simultaneously with the condition $\dot{Q}''_{\mu x} = 0$, the following solutions are obtained:

$$\dot{Q}_{\mu x} = \underline{A}_1 x, \quad (37)$$

$$\delta_x = \delta_0 - \frac{k_1 \alpha_1}{\underline{A}_1^2} \cdot ln(|cos(\beta_1 \underline{A}_1 x)|) \quad (38)$$

$$\dot{U}_{\mu x} = \frac{\underline{A}_1}{k_1}\delta_0 - \frac{k_1}{\underline{A}_1^2} \cdot ln(|cos(\beta_1 \underline{A}_1 x)|). \quad (39)$$

Substituting the third boundary condition given in Eq. (16) into Eq. (37) yields the following third-order algebraic equation with respect to A_1:

$$\frac{k_1 \alpha_1}{\underline{A}_1^2} ln(|cos(\beta_1 \underline{A}_1 X_{\text{м}})|) - \frac{\underline{A}_1}{k_1}\delta_0 - \alpha l_{\mu 0} tg(\beta_1 \underline{A}_1 X_{\text{м}}) + \dot{F}_{exc} = 0 \quad (40)$$

Equation (40) is also a transcendental equation and, therefore, has no exact analytical solution.

It should also be noted that when the primary magnetization curve is approximated by the three-term incomplete polynomial $H = pB + qB^3 + dB^5$, the analytical method proposed in [15] likewise does not yield an exact analytical solution.

Conclusion

In this study, the linear and nonlinear distributed-parameter magnetic circuits (DPMCs) of a newly developed resonant transformer sensor (EMT) intended for the simultaneous conversion of motion parameters (displacement and velocity) into electrical signals were investigated.

The analysis of the linear DPMC showed that both the magnetic flux and the magnetic potential difference are distributed nonlinearly along the magnetic

circuit, and that the degree of this nonlinearity increases with the magnetic field attenuation coefficient.

For the nonlinear DPMC, it was established that a linear distribution of the working magnetic flux along the magnetic circuit can be achieved only if the working air gap between adjacent elongated ferromagnetic rods varies according to a specific law along the circuit length. Furthermore, the distribution of the working magnetic flux is independent of the value of the approximation coefficient characterizing the nonlinear magnetization properties of the magnetic circuit.

It was also found that the magnetic potential difference between adjacent elongated ferromagnetic rods decreases nonlinearly from the region containing the magnetomotive force (MMF) source toward the open end of the magnetic circuit. Moreover, the degree of this decrease increases with increasing values of the approximation coefficient describing the nonlinearity of the magnetic circuit.

References

[1] Kabanov, V.N. Elements of Automation: Textbook. Yekaterinburg: Ural State University of Railway Transport, 2010.

[2] Yusupbekov, N.R., Igamberdiev, H.Z., & Malikov, A.V. Fundamentals of Automation of Technological Processes. Textbook. Vols. 1–2. Tashkent: Tashkent State Technical University, 2007.

[3] Polishchuk, E.S., et al. Instruments and Methods for Measuring Non-Electrical Quantities. Edited by E.S. Polishchuk. Beskid-BT, 2008.

[4] Fedotov, A.V. Theory and Design of Inductive Displacement Sensors for Automatic Control Systems. Omsk: Omsk State Technical University Publishing House, 2011.

[5] Sharapov, V.M., & Polishchuk, E.S. (Eds.). Sensors: Reference Handbook. Moscow: Technosphere, 2012.
[6] Zudin, V.L., Zhukov, Yu.P., & Malanov, A.G. Sensors: Measurement of Displacement, Deformation and Force. 2nd ed. Moscow: Yurait Publishing House, 2024.
[7] Rannev, G.G. (Ed.). Information and Measurement Technology and Electronics. Moscow: Akademiya, 2007.
[8] Amirov, S.F., Sharapov, Sh.A., Sulliev, A.Kh., Boltaev, O.T., & Karimov, I.A. Transformer Sensor for Large Linear Displacements with Enhanced Sensitivity. Patent of the Republic of Uzbekistan No. IAP 7953, 2023.
[9] Amirov, S.F., Sulliev, A.Kh., Norjigitov, S.A., Fayzullaev, J.S., & Mukhtorov, U.B. Motion Parameter Sensor. Patent of the Republic of Uzbekistan No. IAP 8090, 2025.
[10] Zaripov, M.F. Distributed-Parameter Sensors for Automation and Information Measurement Technology. Moscow: Energiya, 1969.
[11] Konyukhov, N.E., Mednikov, F.M., & Nechaevskii, M.L. Transformer Sensors for Mechanical Quantities. Moscow: Mashinostroenie, 1987.
[12] Amirov, S.F., Sulliev, A.Kh., & Balgaev, N.E. A brief review of methods for calculating distributed-parameter magnetic circuits. Problems of Energy and Resource Saving, 2010, No. 1–2, pp. 195–202.
[13] Fayzullaev, J.S. Comparative analysis of methods for investigating nonlinear distributed-parameter magnetic circuits. Railway Transport: Current Challenges and Innovations, 2025, No. 2, pp. 151–162.
[14] Bronshtein, I.N., & Semendyaev, K.A. Handbook of Mathematics for Engineers and Engineering Students. Saint Petersburg: Lan Publishing House, 2010.

[15] Fayzullaev, J.S. Investigation of nonlinear magnetic circuits of measuring sensors with a special distributed-parameter structure. Chemical Technology. Control and Management, 2025, No. 6, pp. 22–36.
[16] Matyuk, V.F., & Osipov, A.A. Mathematical models of the magnetization curve. Non-Destructive Testing and Diagnostics, 2011, No. 2, pp. 3–20.
[17] Zubkov, Yu.V. Approximation of magnetization curves of electrical steel in the design of integrated electromechanical sensors. Proceedings of Higher Educational Institutions. Electromechanics, 2007, No. 6, pp. 19–22.
[18] Aliev, I.I., & Kalganova, S.K. Electrical Engineering Materials and Products: Reference Book. Moscow: RadioSoft, 2005.
[19] Fayzullaev, J.S. Approximation functions of the magnetization curve and their application to the analysis of nonlinear distributed-parameter magnetic circuits. Railway Transport: Current Challenges and Innovations, 2025, No. 2, pp. 218–229.